Nuclear receptor REV-ERBα mediates circadian sensitivity to mortality in murine vesicular stomatitis virus-induced encephalitis

Khatuna Gagnidze[a,b], Kaitlyn H. Hajdarovic[a,b], Marina Moskalenko[a,b], Ilia N. Karatsoreos[c], Bruce S. McEwen[b,1], and Karen Bulloch[a,b,1]

[a]Neuroimmunology and Inflammation Program, The Rockefeller University, New York, NY 10065; [b]Harold and Margaret Milliken Hatch Laboratory of Neuroendocrinology, The Rockefeller University, New York, NY 10065; and [c]Department of Integrative Physiology and Neuroscience, Washington State University, Pullman, WA 99164

Contributed by Bruce S. McEwen, March 24, 2016 (sent for review October 16, 2015; reviewed by Lance J. Kriegsfeld and Randy J. Nelson)

Certain components and functions of the immune system, most notably cytokine production and immune cell migration, are under circadian regulation. Such regulation suggests that circadian rhythms may have an effect on disease onset, progression, and resolution. In the vesicular stomatitis virus (VSV)-induced encephalitis model, the replication, caudal penetration, and survivability of intranasally applied VSV depends on both innate and adaptive immune mechanisms. In the current study, we investigated the effect of circadian time of infection on the progression and outcome of VSV-induced encephalitis and demonstrated a significant decrease in the survival rate in mice infected at the start of the rest cycle, zeitgeber time 0 (ZT0). The lower survival rate in these mice was associated with higher levels of circulating chemokine (C-C motif) ligand 2 (CCL2), a greater number of peripherally derived immune cells accumulating in the olfactory bulb (OB), and increased production of proinflammatory cytokines, indicating an immune-mediated pathology. We also found that the acrophase of molecular circadian clock component REV-ERBα mRNA expression in the OB coincides with the start of the active cycle, ZT12, when VSV infection results in a more favorable outcome. This result led us to hypothesize that REV-ERBα may mediate the circadian effect on survival following VSV infection. Blocking REV-ERBα activity before VSV administration resulted in a significant increase in the expression of CCL2 and decreased survival in mice infected at the start of the active cycle. These data demonstrate that REV-ERBα–mediated inhibition of CCL2 expression during viral-induced encephalitis may have a protective effect.

circadian | inflammation | immune response | monocytes | vesicular stomatitis virus

Circadian rhythms are daily oscillations of physiological and behavioral parameters driven by the suprachiasmatic nucleus (SCN), the "master clock" of the organism, through humoral and neural outputs (1). At the molecular level, the clock is comprised of at least three interlocking transcription loops, which regulate circadian oscillations in gene expression within the cell (1). In the immune system, intrinsic clocks have been identified in various cell lineages, including macrophages, lymphocytes, and microglia (1–3). Direct control of immune gene expression, among them proinflammatory cytokines, by the clock transcription factors BMAL and REV-ERBα also has been demonstrated (4–7). Furthermore, some of the functional aspects of immune cells, such as the rate of phagocytosis, lymphocyte proliferation, and cytolytic activity, are under circadian control (8–10). The migration of hematopoietic progenitors and mature leukocytes also displays daily variation, which can be particularly consequential to disease outcomes (1–3, 11, 12).

Monocytes are bone marrow-derived cells characterized by Ly6c^{hi}/ CCR2^{hi} expression, which are recruited to the sites of infection and injury, including those occurring in the CNS (2, 3, 13, 14). These cells have the capacity to differentiate into macrophages and dendritic cells (DC), perform effector functions such as antigen presentation and T-cell stimulation, and produce proinflammatory cytokines and chemokines, all directed to contain and clear infection (8, 9, 13, 15). However, poorly controlled migration of these cells may result in immune-mediated pathology and tissue damage, as has been shown for stroke, experimental autoimmune encephalomyelitis (EAE), and traumatic brain injury (16–18).

Intranasal (i.n.) vesicular stomatitis virus (VSV) infection is a well-established murine encephalitis model. A single application of VSV leads to infection and viral replication within sensory neurons in the neuroepithelium. Within 12–24 h the virus is transported to the olfactory bulb (OB) via the olfactory nerve, spreads through deeper layers, and reaches the olfactory ventricle 4 d postinfection (dpi). The virus spreads retrograde via olfactory circuits and along the ventricular system and reaches the hindbrain by 8 dpi (19). By 4 dpi VSV infection also leads to the accumulation of a mixed cellular infiltrate in the OB containing brain-resident microglia (MG) and dendritic cells (bDC) as well as CD45^{hi}/CD11b^{hi} and CD45^{hi}/CD11b^{int} cells of peripheral origin (20). In the current study, we tested the hypothesis that the immune response to VSV is under circadian control and examined the molecular and cellular immune mechanisms underlying such circadian regulation. We observed that the poor survival rate of mice infected at the beginning of the rest cycle [zeitgeber time 0 (ZT0)] (hereafter "ZT0 mice) was associated with higher levels of circulating chemokine (C-C motif) ligand 2 (CCL2), a proinflammatory chemokine, and a greater proportion of infiltrating CD45^{hi}/CD11b^{hi} and CD45^{hi}/CD11b^{int} cells, identified as

Significance

Immune parameters exhibit circadian periodicity. We show that disease progression and survival following intranasal infection with a neurotropic virus depends on the circadian time of infection. Infection occurring at the start of the rest period leads to higher mortality than infection at the start of the active period and is associated with increased numbers of inflammatory cells and higher levels of chemokine (C-C motif) ligand 2 (CCL2). The highest expression of REV-ERBα, a component of the molecular circadian clock, coincides with the start of the active cycle, when vesicular stomatitis virus infection leads to lower mortality. Inhibiting REV-ERBα–mediated suppression of CCL2 at the start of the active cycle abolishes protection in these animals, thus providing insight into circadian regulation of immune response.

Author contributions: K.G. and K.B. designed research; K.G., K.H.H., and M.M. performed research; K.G., K.H.H., M.M., I.N.K., B.S.M., and K.B. analyzed data; and K.G., I.N.K., B.S.M., and K.B. wrote the paper.

Reviewers: L.J.K., University of California, Berkeley; and R.J.N., The Ohio State University College of Medicine.

The authors declare no conflict of interest.

[1]To whom correspondence may be addressed. Email: mcewen@rockefeller.edu or bulloch@mail.rockefeller.edu.

This article contains supporting information online at www.pnas.org/lookup/suppl/doi:10.1073/pnas.1520489113/-/DCSupplemental.

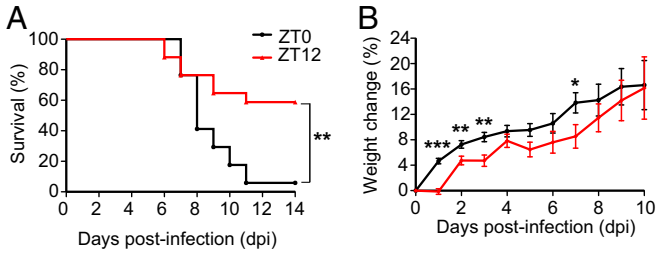

Fig. 1. Circadian time of infection affects survival following VSV i.n. administration. Two groups of mice were maintained on opposite light–dark cycles. For one group of mice VSV infection (LD_{50} dose applied i.n.) was done at the start of the light cycle (ZT0), and for the other group i.n. VSV application was done at the start of dark cycle (ZT12). (*A*) Survival curves are a composite of three independent experiments [total $n = 17$ per group, log-rank (Mantel–Cox) test, $P = 0.004$]. (*B*) Disease progression is expressed as the percent of weight change following VSV infection. Compiled data are expressed as mean ± SEM (total $n = 17$ per group; Student's t test, $^{*}P < 0.05$, $^{**}P < 0.01$, $^{***}P < 0.001$).

proinflammatory monocytes, in the OB. Pretreatment of VSV-infected mice with a REV-ERBα antagonist (SR8278) resulted in a significant increase in CCL2 mRNA expression in mice infected at ZT12 (hereafter "ZT12 mice") and a decrease in their survival. These data demonstrate that REV-ERBα–mediated inhibition of CCL2 expression during viral-induced encephalitis may have neuroprotective effects and hence improve survival.

Results

Circadian Time of Infection Affects Disease Progression and Survival. To test the hypothesis that the circadian time of infection impacts VSV-induced encephalitis, two groups of male mice, maintained on opposing light:dark cycles, were infected either at the start of the active period (ZT12) or at the end of the active period (ZT0). Disease progression (measured by weight loss) and the mortality rate of the animals were monitored daily for 2 wk following the infection. We found that viral infection at ZT12 resulted in a 40% mortality rate, as expected with an LD_{50} dose. The same dose of virus administered at ZT0 led to a 95% mortality rate (Fig. 1*A*). Consistent with the poor survival rate, mice infected at ZT0 lost a higher percentage of body weight than mice infected at ZT12, and the differences were most pronounced during the first 4 dpi (Fig. 1*B*). These data demonstrate that animals are more susceptible to VSV-induced encephalitis at the end of their active cycle (ZT0) and indicate circadian/diurnal regulation of the antiviral response.

Immune Response to i.n. VSV Infection Is Initiated in the Periphery. To examine the inflammatory response elicited by VSV i.n. administration at two circadian time points, we measured circulating cytokine levels after infection. Two groups of mice were infected at either ZT0 or ZT12, and blood samples were collected 12, 24, 48, 72, or 96 h postinfection (hpi). Control mice were treated with PBS solution (the vehicle for VSV), and blood samples were collected 96 h posttreatment. Levels of IFNγ, IL-6, and CCL2 in the blood of VSV-infected mice were elevated significantly at 24 hpi (Fig. 2 *A*–*C* and Table S1). IFNγ and IL-6 returned to baseline (the level in the PBS-treated cohort) at 48 hpi, but CCL2 levels were sustained and declined only at 72 hpi. Moreover, the magnitude of cytokine increase was different in the two circadian groups: ZT12 mice had higher levels of IFNγ at 24 hpi, and ZT0 mice had higher CCL2 at 48 hpi (Fig. 2 *A*–*C* and Table S1). Moderate but significant changes were detected in the levels of TNF and IL12p70 following VSV infection, but IL-10 levels were not affected (Fig. S1 and Table S1). Together these data demonstrate that the systemic immune response to i.n. VSV infection is very rapid and depends on the circadian time of infection.

In addition to proinflammatory cytokines, we measured levels of circulating corticosterone (CORT), an antiinflammatory hormone that displays circadian oscillation and mediates synchronization of peripheral clocks. CORT levels were measured in blood samples collected from ZT0 and ZT12 mice under baseline (PBS-treated) conditions and at 24, 48, 72, or 96 h following VSV infection (Fig. 2*D*). As expected, CORT levels in PBS-treated control mice were higher at ZT12 than at ZT0. Following VSV i.n. administration, mice infected at ZT12 maintain CORT levels comparable to those in controls at 24, 48, 72, and 96 hpi. In contrast CORT levels in mice infected at ZT0 are significantly increased at 24 hpi and return to the basal (PBS-treated) level by 48–72 hpi (Fig. 2*D* and Table S1). These data indicate that VSV infection affects CORT secretion in mice infected at ZT0 and that this effect may contribute to neuroinflammation and the poor survival of these mice.

VSV administered i.n. travels not only to the brain but also to the lung, spleen, and cervical lymph nodes (21, 22). Thus, to characterize the whole-body immune response elicited by the virus, we examined the circadian regulation of the peripheral immune response mounted in the lung and spleen. We found that mRNA levels of the proinflammatory cytokines IL-6, IFNγ, and CCL2 are elevated by 24 hpi in the spleen and lung tissue of mice infected at ZT0 and ZT12 (Fig. S2*A* and *B*) and that this elevation coincides with the rise of inflammatory cytokines in blood (Fig. 2 *A*–*C*). Our data also showed that Toll-like receptor 7 (TLR7), TLR9, and MyD88 mRNA expression is uniquely induced in the lung but not in the spleen at the same time point (Fig. S2*A* and *B*).

Proinflammatory Monocytes Accumulate in the OB of VSV-Infected Mice. We next examined whether the circadian time of infection affects the cellular response to VSV in mice infected at ZT0 and ZT12. As described previously (20), cell populations isolated from VSV-infected OB contain brain-resident MG ($CD45^{int}/CD11b^{hi}/CD11c^{-}$) and bDC ($CD45^{int}/CD11b^{hi}/CD11c^{+}$) (Fig. 3*A* and Fig. S3*B*). A time-course analysis of VSV infection also revealed that by 72 hpi two additional cell populations, $CD45^{hi}/CD11b^{hi}$ and $CD45^{hi}/CD11b^{int}$, accumulated in VSV-infected OB (Fig. S3*B*), and

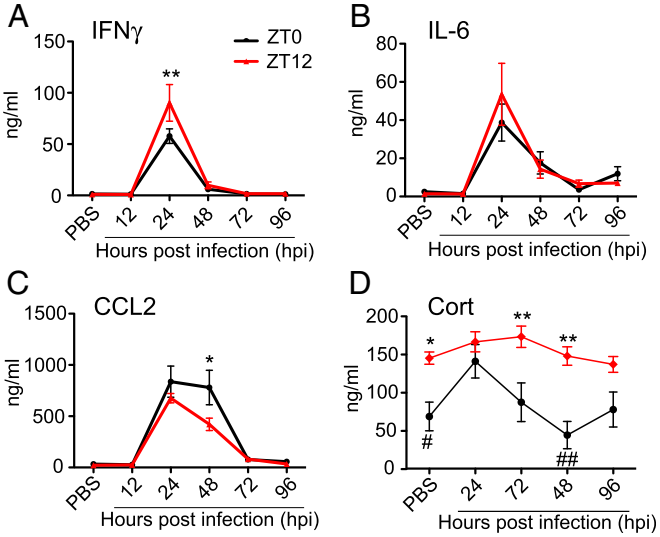

Fig. 2. Circadian time of infection affects cytokine and hormone levels following VSV i.n. administration. Blood samples were collected from ZT0 and ZT12 mice under the control (PBS-treated) condition and at the indicated time points following VSV infection. (*A*–*C*) Circulating cytokine levels were measured using cytometric bead array. Data compiled from two independent experiments are expressed as mean ± SEM (total $n = 6$ per time point, two-way ANOVA, Bonferroni's posttest; $^{*}P < 0.05$, $^{**}P < 0.01$, ZT12 vs. ZT0). (*D*) Blood CORT levels were measured by RIA. Data compiled from two independent experiments are expressed as mean ± SEM (total $n = 6$ per time point; two-way ANOVA, Bonferroni's posttest, $^{*}P < 0.05$, $^{**}P < 0.01$, ZT12 vs. ZT0; comparison within each circadian group was done using Student's t test, $^{\#}P < 0.05$, $^{\#\#}P < 0.001$ vs. ZT0 acrophase).

NEUROSCIENCE

the proportion of these cells at 96 hpi was significantly higher in mice infected at ZT0 than in mice infected at ZT12 (Fig. 3*A*).

To understand better the role of the $CD45^{+}/CD11b^{+}$ cell populations in VSV-induced pathology, we examined the phenotype of these cells using flow cytometry (Fig. 3 *B–D*). We found that $CD45^{hi}/CD11b^{hi}$ cells [previously shown to be peripherally derived (20)] are Gr-1^{hi}, $Ly6c^{hi}$, $CCR2^{+}$, $F4/80^{+}$, $CD11c^{+}$, and MHC II^{+}. These cells also express the costimulatory molecules CD86 and CD80 and markers for specialized DC subsets, CD103 and B220. These data indicate that $CD45^{hi}/CD11b^{hi}$ cells contain proinflammatory monocytes as well as effector DC and macrophage subpopulations. Analysis of the $CD45^{hi}/CD11b^{int}$ population also revealed the presence of $CD11c^{+}$, $NK1.1^{+}$, $B220^{+}$ cells, which resemble IFN-producing killer DCs. Moreover, $CD45^{hi}/CD11b^{int}$ cells contain a $Ly6c^{+}$ subpopulation, indicating a monocytic lineage. Notably, no phenotypic differences were found among immune cell populations derived from ZT0 and ZT12 mice.

To examine the subpopulations of effector DCs and macrophages, which derive from proinflammatory monocytes, we next examined $CD11c^{+}$ and $CD11c^{-}$ subsets within CD45/CD11b cells. We found that $CD45^{hi}/CD11b^{hi}$ cells isolated from ZT12 VSV-infected mice contained a significantly higher proportion of $CD11c^{+}$ cells and a significantly lower proportion of $CD11c^{-}$ cells compared with $CD45^{hi}/CD11b^{hi}$ cells from ZT0 mice (Fig. S4*A*). No difference in the numbers of $CD11c^{+}$ and $CD11c^{-}$ cells was found among other cell subsets in either ZT0 or ZT12 mice. Further phenotyping of $CD45^{hi}/CD11b^{hi}/CD11c^{+}$ and $CD45^{hi}/CD11b^{hi}/CD11c^{-}$ cells also revealed that $CD11c^{+}$ cells display a more activated phenotype and express higher levels of MHC II and the costimulatory molecules CD86 and CD40, as is consistent with the phenotype of monocyte-derived DCs (Fig. S4*B*). These data indicate that the disproportional accumulation of proinflammatory and effector cells in the OB of VSV-infected mice is influenced by the time of infection.

VSV Infection Leads to Up-Regulation of Cytokines in the OB 96 hpi. We next examined whether the time of VSV infection affects the level of proinflammatory cytokine mRNA expression in the OB tissue at 12, 24, 48, 72, and 96 hpi. We found that i.n. VSV inoculation led to up-regulation of all genes examined by 48–72 hpi and reached significantly high levels at 96 hpi (Fig. 4 and Table S2). At the same time points, mice infected at ZT0 displayed significantly higher levels of IL1β, IL-6, TNF, IFNγ, and CCL2 mRNA expression than mice infected at ZT12 (Fig. 4 *A–E*). We also found that the expression of various antiviral factors and pattern-recognition receptors was elevated in the OB of VSV-infected mice at 96 hpi and that the expression of these factors and receptors was consistently higher in the OB of ZT0 mice than in the OB of ZT12 mice (Fig. S5 and Table S2). These data indicate that the circadian time of infection affects the changes in proinflammatory gene expression induced by VSV inoculation.

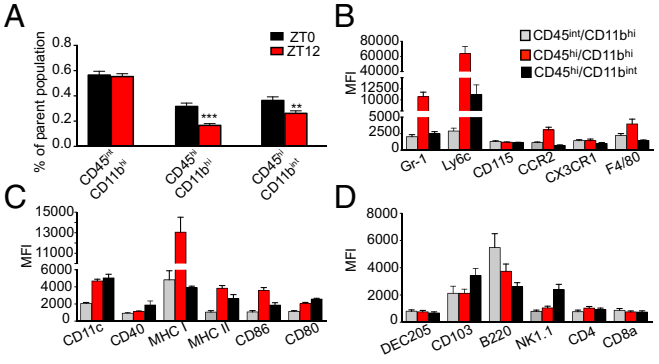

Fig. 3. Circadian time of infection affects immune cell populations in the OB of VSV-infected mice. Mice were killed at 96 h following VSV, and OB tissue was processed for flow cytometry analysis. (*A*) Cells pregated on live/singlets/lin^{-} were analyzed based on the expression of CD45 and CD11b. Three distinct populations were detected: $CD45^{int}/CD11b^{hi}$, $CD45^{hi}/CD11b^{hi}$, and $CD45^{hi}/CD11b^{int}$. Compiled data are expressed as mean ± SEM of the percent of parent population (n = 50 for each population; Student's t test, $^{**}P < 0.01$, $^{***}P < 0.001$, ZT12 vs. ZT0). (*B–D*) CD45/CD11b cell populations were phenotyped using flow cytometry. Only data for ZT0 group are shown because no phenotypic differences were found between the ZT0 and ZT12 groups. Data compiled from two or three independent experiments are expressed as mean ± SEM of geometric mean of fluorescence intensity (MFI) for each antibody (total n = 4–6 per group.)

Expression of Circadian Clock Genes in the Steady-State OB. To identify the factors responsible for the circadian effect on VSV-induced encephalitis, we analyzed the expression of clock genes in the OB tissue of naive mice. Analysis of mRNA levels at four different time points—ZT0, ZT6, ZT12, and ZT18—revealed that BMAL, Per2, Cry1, and Rev-ERBα mRNA levels displayed rhythmic changes over the 24-h time period; however CLOCK and RORα mRNA did not (Fig. 5). Furthermore, significant differences between ZT0 and ZT12 time points were detected in the transcript levels of BMAL, Cry1, and Rev-ERBα, with BMAL and Cry1 mRNA displaying a lower expression and Rev-ERBα mRNA showing higher expression at ZT12 (Fig. 5). Notably, this expression pattern of REV-ERBα mRNA in the OB tissue appears to be antiphase with its expression in the SCN (23). However, this pattern is not surprising in light of evidence that the OB represents a functional circadian pacemaker that is capable of producing autonomous and entrainable rhythms independent of the SCN (24).

We also analyzed the daily variation in the expression of various immune genes involved in pattern recognition (Fig. S6 *A–F*), inflammation and antiviral response (Fig. S6 *G–L*), and cell migration (Fig. S6 *M–Q*). We found no significant differences in the mRNA levels of the examined genes across time points in the uninfected mice. However, slight time-of-day variations in the mRNA expression levels of TLR7, IL1β, IFNβ, IFNAR1 and IFNAR2, CCL2, and CCL3 were detected.

REV-ERBα Mediates the Circadian Effect on Survival Following VSV i.n. Administration. Differences detected in the expression of REV-ERBα in the OB tissue between the ZT0 and ZT12 time points led us to hypothesize that the circadian difference seen in VSV-induced encephalitis may be mediated by REV-ERBα. To test this hypothesis, we used a synthetic antagonist for REV-ERBα, SR8278, to block the activity of the receptor in the OB of VSV-infected mice. This compound has been shown to alter the mRNA levels of REV-ERBα target genes in vitro and in vivo and to produce behavioral changes in mice following microinfusion into the ventral midbrain (25, 26). We administered two doses of SR8278 i.n., the first 4 h before infection and the second concomitant with VSV i.n. administration. To account for the drug-only effect, we also treated groups of mice with the SR8278/PBS combination. We found that blocking REV-ERBα activity in mice infected with VSV at the start of their active phase (ZT12) significantly reduced the survival rate compared with vehicle-treated ZT12 mice (Fig. 6*A*). In contrast, SR8278 treatment had no effect on the survival of VSV-infected versus vehicle-treated ZT0 mice (Fig. 6*A*). SR8278 had no effect on the health and survival of PBS-treated mice (Fig. S7*A*).

To explore the molecular mechanism of the effect of REV-ERBα on VSV-induced mortality, we measured the expression of REV-ERBα target genes as well as clock genes following treatment with SR8278 or vehicle. It has been demonstrated that i.n. delivery of compounds could spread to lung tissue as well as the OB; therefore we selected these two sites for the analysis (27, 28). Blocking REV-ERBα activity with SR8278 led to a significant up-regulation of CCL2 mRNA 12 h posttreatment in the OB tissue of ZT12 mice, compared with vehicle-treated ZT12 mice (Fig. 6*B*). No effect on the mRNA expression of IL-6, BMAL, or any other clock genes was found in the OBs of either ZT0 or ZT12 mice (Fig. 6*B* and Fig. S7*B*). In contrast, changes in the expression levels of RORα (decreased) and IL-6 (increased) mRNA were found in the lung tissue of ZT0 mice (Fig. S7*C*). These changes did not affect the survival

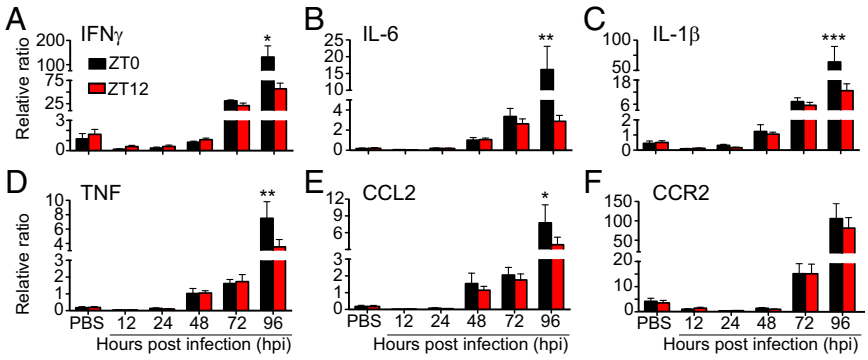

Fig. 4. Circadian time of infection affects gene expression in the OB of VSV-infected mice. Total RNA was isolated from OB tissue of VSV-infected mice at the indicated time points. Transcript levels for proinflammatory cytokines (*A*–*D*); chemokine (*E*), and chemokine receptor (*F*) were measured by qPCR. Data compiled from two independent experiments are expressed as mean ± SEM (n = 6–8 per time point; two-way ANOVA, Bonferroni's posttest, $*P < 0.05$, $**P < 0.01$, $***P < 0.001$, ZT0 vs. ZT12).

rate of the animals. These data suggest that REV-ERBα–mediated circadian effect on CCL2 expression in the OB affects the immune response to VSV-induced encephalitis and the survival of the animal.

CCL2 Is Expressed in Resident and Infiltrating Cells of the OB. To identify the cellular source of CCL2 in the OB, we examined the expression levels of CCL2 mRNA in cell populations isolated from OB of naive and VSV-infected mice using FACS. We found that brain-resident MG and bDC both express low levels of CCL2 mRNA in steady state (Fig. 7*A*). VSV infection induces CCL2 mRNA expression at 96 hpi only in bDCs isolated from ZT12 mice. Interestingly, two cell populations that infiltrate the OB of VSV-infected mice at 96 hpi, $CD45^{hi}/CD11b^{hi}$ and $CD45^{hi}/CD11b^{int}$, display drastically different levels of CCL2 mRNA expression: Both $CD11c^{+}$ and $CD11c^{-}$ cells within the $CD45^{hi}/CD11b^{hi}$ population express high levels of CCL2 mRNA, and the expression level is higher in mice infected at ZT12. In contrast, only the $CD45^{hi}/CD11b^{int}/CD11c^{-}$ cells isolated from ZT0 mice display CCL2 expression; no CCL2 mRNA was detected in cells isolated from ZT12 mice (Fig. 7*A*).

The expression pattern of CCR2 mRNA in the sorted cell populations (Fig. 7*B*) was in agreement with our flow cytometry data (Fig. 3*B*): (*i*) the $CD45^{int}/CD11b^{hi}$ population expresses low levels of CCR2 in steady state and following VSV challenge, and (*ii*) both $CD11c^{+}$ and $CD11c^{-}$ subpopulations of $CD45^{hi}/CD11b^{hi}$ and $CD45^{hi}/CD11b^{int}$ cells express high levels of CCR2 96 h following VSV. Interestingly, differences were observed in the levels of CCR2 mRNA in the $CD45^{hi}/CD11b^{hi}$ cell subpopulation isolated from ZT0 and ZT12 mice; however these differences were not reflected in the cell-surface expression of CCR2 as seen by flow cytometry (Fig. S4*B*).

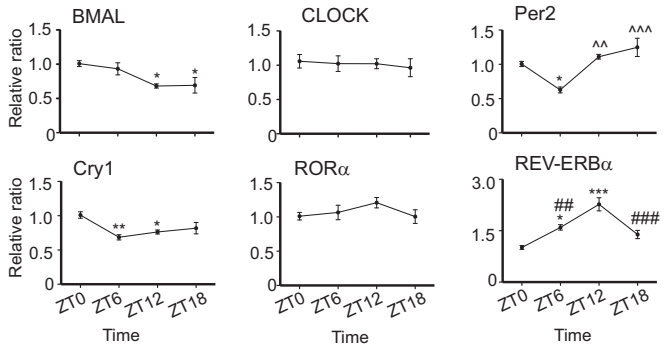

Fig. 5. Expression of circadian clock genes in the OB tissue of naive mice. Total RNA was isolated from OB tissue at the indicated time points. Transcript levels for circadian clock genes were measured by qPCR. Data compiled from three independent experiments are expressed as mean ± SEM (total n = 6 per time point; one-way ANOVA, Bonferroni's posttest, $*P < 0.05$, $**P < 0.01$, $***P < 0.001$ vs. ZT0; $\wedge\wedge P < 0.01$, $\wedge\wedge\wedge P < 0.001$ vs. ZT6; $^{\#\#}P < 0.01$, $^{\#\#\#}P < 0.001$ vs. ZT12).

To confirm further the source of CCL2 in the VSV-infected OB, we examined the expression of CCL2 in OB tissue obtained from control and VSV-treated mice. Double immunolabeling for CCL2 and cell markers for MG (IbaI) (Fig. S8*A*), astroglia (GFAP) (Fig. S8*B*), and neurons (TUJ-1) (Fig. S8*C*) was performed. We found that both $Iba1^{+}$ MG and $GFAP^{+}$ astrocytes express CCL2 at 96 h following VSV i.n. administration. Moreover, in the CD11c-EYFP transgenic mouse OB we also detected colocalization of CCL2 with $EYFP^{+}$ bDCs (Fig. S8*A*). Little or no CCL2 expression was detected in mitral cells of the OB, but diffuse labeling of CCL2 was evident in the granule cell layer of the OB (Fig. S8*C*).

Discussion

Our results demonstrate that the circadian time of infection has a significant effect on the development and resolution of VSV-induced encephalitis. Specifically, we found that viral inoculation applied at the end of the active cycle (ZT0) leads to poor survival and is associated with a higher level of circulating CCL2 and a higher proportion of $CD45^{hi}/CD11b^{hi}$ and $CD45^{hi}/CD11b^{int}$ cells (identified as inflammatory monocytes) in the OB. We also have demonstrated that relieving REV-ERBα–mediated inhibition of CCL2 mRNA expression using receptor antagonist treatment during virus-induced encephalitis results in decreased survival.

The circadian effect on immune response has been demonstrated in number of infection models, including LPS-induced inflammation, pneumococcal infection, and cecal ligation puncture (CLP)-induced sepsis (1, 4, 12, 14). It is noteworthy that the acrophase of the circadian effect in each of these experimental models falls at different times in the daily cycle, suggesting differential underlying mechanisms. For example, clearance of *Streptococcus pneumoniae* from the lung depends on the circadian variation in the expression of CXCL5 and subsequent neutrophil recruitment (12), whereas circadian expression of TLR9 in mouse spleen determines the severity of response in CLP-induced sepsis (4).

Cytokines, chemokines, and hormones, which are critical regulators of immune function, also display circadian oscillation. For example, the induction of IL-6, IL-12 (p40), CCL2, and CCL5 in circulation and peritoneal exudate cells is far greater in mice challenged with LPS at ZT12 than at ZT0 (7). In our study, we also found that the VSV-induced increase in circulating inflammatory cytokines depends on the time of infection, with IFNγ and IL-6 levels being higher in mice infected at ZT12 and the level of CCL2 being higher and more sustained in mice infected at ZT0. It is noteworthy that we have not identified the specific source of the circulating cytokines following VSV challenge. However, we found the up-regulation of proinflammatory cytokine mRNA in the spleen and lung tissues of infected mice at the same time point (24 hpi) as increases in blood cytokine levels, suggesting that spleen and/or lung immune cells may be the source of circulating "alert" cytokines at this early stage of infection. These data are in agreement with a previous report that the infectious VSV is transiently present in lungs and spleens at 24 hpi (21) and may be able to initiate peripheral immune responses.

It must be noted that our experimental paradigm, which required having the measures for time-course experiments taken 12 h out of

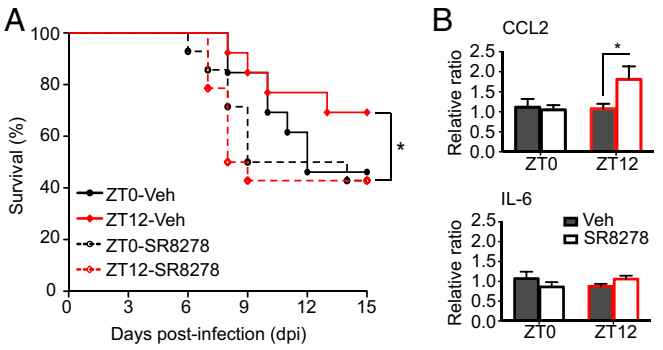

Fig. 6. Inactivation of REV-ERBα during VSV i.n. administration leads to poor survival. Two groups of mice were treated i.n. with either SR8278 (20 μg) or with vehicle solution administered twice: 4 h before and concomitant with VSV infection. (*A*) Survival curves are a composite of two independent experiments [total $n = 13$ per group; log-rank (Mantel–Cox) test, $*P = 0.047$ for ZT12-vehicle vs. ZT12-SR8278). (*B*) Total RNA was isolated from OB tissue of SR8278- or vehicle-treated mice 12 h after VSV i.n. administration. Transcript levels for CCL2 and IL-6 were measured by qPCR. Data compiled from two independent experiments are expressed as mean ± SEM (total $n = 5$ per time point; two-way ANOVA, Bonferroni's posttest, $*P < 0.05$, ZT12-vehicle vs. ZT12-SR8278).

phase between groups, may have impacted data interpretation in cases where parameters showed circadian fluctuations. However, most measures taken (circulated cytokines, mRNA levels, cell numbers) displayed differences between two circadian groups only at specific time points (being comparable at all other time points), allowing us to conclude that circadian variation at the time of sample collection was not a significant factor for data interpretation.

Reciprocal regulation between cytokines and glucocorticoids has been described in various infection models: Pathogen-induced cytokines increase CORT production, which through a negative feedback loop down-regulates cytokine levels and attenuates inflammation (29, 30). We found that CORT levels are differentially affected by VSV, depending on the time of infection. In mice infected at the end of the active cycle (ZT0, the nadir of CORT), we observed an increase in the blood CORT levels coinciding with an increase in circulating cytokines at 24 hpi. In contrast, mice infected at the start of the active cycle (ZT12, the acrophase of CORT) maintained stable CORT levels for the following 96 hpi (measured daily at ZT12). Thus, CORT, acting through the glucocorticoid receptor and antagonizing NF-κB, may limit cytokine expression in ZT12 mice (31). It has been long recognized that acute stress and the associated surge in glucocorticoid levels result in a decrease in blood monocyte numbers (32) and have a protective effect during immune challenge (33). Our data showing a lower proportion of monocytes accumulating in the OB and better survival of mice infected at the peak of endogenous CORT at ZT12 are in accordance with these previous findings.

Monocyte infiltration is an important step in the defense against pathogens. However, uncontrolled accumulation of these cells at the site of infection, particularly in the CNS, may lead to immune-mediated pathology and irreparable tissue damage as seen in viral encephalitis models, stroke, traumatic brain injury, and EAE (13, 16–18, 34). In the current study we identified the $CD45^{hi}/CD11b^{hi}/Ly6c^{hi}/CCR2^{+}$ cell population accumulating in the OB following VSV infection as proinflammatory monocytes. Notably, greater numbers of these cells and higher levels of proinflammatory cytokines, characteristics of an overactive immune response, were detected in the OB of mice infected at the end of the active cycle (ZT0), and these mice also were more susceptible to virus-induced mortality. At the same time, the amounts of virus present in the OB of mice infected with VSV at either ZT0 or ZT12 did not differ (Fig. S9). These data point to circadian regulation of monocyte trafficking into the brain and the critical role these cells may play in immune-mediated pathology.

The chemokine ligand CCL2 and its receptor CCR2 are the critical signaling factors that mediate monocyte egress from bone marrow and recruitment to the site of infection (14, 35). Interfering with CCR2–CCL2 signaling by means of genetic modification or pharmacological agents has a protective effect in a number of inflammatory conditions in both the periphery and the CNS (13, 14, 16). Previously, BMAL was shown to regulate CCL2 expression in $Ly6c^{hi}$ monocytes, and REV-ERBα was implicated in the regulation of CCL2 expression in peritoneal macrophages (5, 8, 11). We found that VSV-induced up-regulation of CCL2 is under circadian control, with mice infected at ZT0 displaying higher levels of CCL2 in circulation and in the OB tissue. To identify the factor(s) involved in the circadian regulation of CCL2, we focused on REV-ERBα for two reasons: (*i*) REV-ERBα has been shown to regulate the expression of two critical proinflammatory factors, CCL2 and IL-6 (5, 6), and (*ii*) we have found that the acrophase of REV-ERBα mRNA expression in the OB is at ZT12 and coincides with the acrophase of survival following VSV infection.

Using a REV-ERBα antagonist 4 h before and concomitantly with VSV i.n. administration led to decreased survival of ZT12 mice and was accompanied by the increased production of CCL2 mRNA in the OB. At present we cannot exclude the possibility that SR8278 also may have effects elsewhere in the brain that then could feed back or forward to the OB. Surprisingly, we did not find that the REV-ERBα antagonist had an effect on the survival or OB gene expression in ZT0 animals, although we did detect increased expression of IL-6 mRNA and decreased expression of RORα mRNA in the lung tissue of SR8278-treated ZT0 mice. We hypothesize that the efficiency of antagonist action may depend on the level of REV-ERBα expression at the time of treatment; hence the lack of response in the OB of ZT0 animals may be caused by a low level of REV-ERBα expression at the time of treatment.

Together these data suggest that (*i*) the effect of blocking REV-ERB activity depends on circadian/diurnal fluctuation in

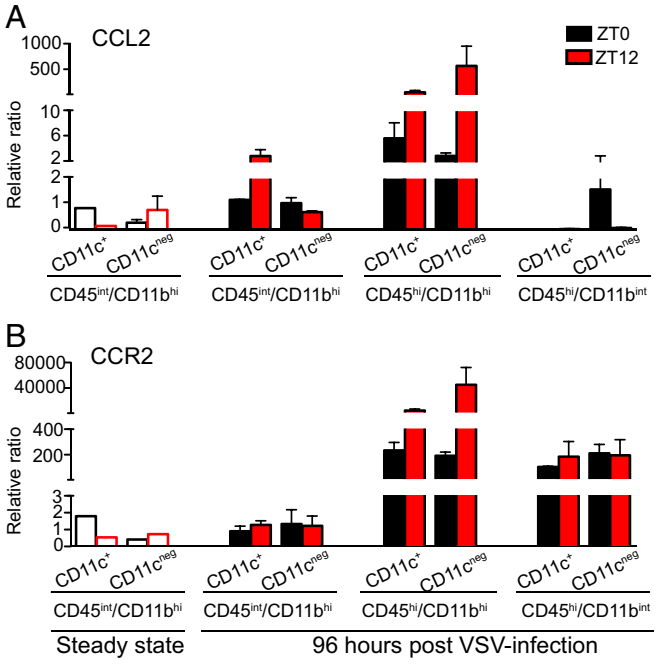

Fig. 7. CCL2 and CCR2 expression in OB immune cells. (*A* and *B*) $CD45^{int}/CD11b^{hi}$, $CD45^{hi}/CD11b^{hi}$, and $CD45^{hi}/CD11b^{int}$ cells isolated from the OB of VSV-infected mice at 96 hpi were FACS sorted based on CD11c expression. The only population present in the OB of untreated mice, $CD45^{int}/CD11b^{hi}$, was analyzed also (steady state, open bars). Total RNA was isolated, and transcript levels for CCL2 (*A*) and CCR2 (*B*) were measured by qPCR. Data compiled from five independent experiments are expressed as mean ± SEM (total $n = 5$).

its expression level, and (*ii*) REV-ERBα–mediated regulation of CCL2 expression affects VSV-induced neuroinflammation, possibly through monocyte migration. Thus, this study reveals a previously unidentified physiological regulatory mechanism underlying disease progression and survival in virus-induced encephalitis and a potential target for therapeutic amelioration of similar viral CNS infections.

Materials and Methods

Mouse Models. All experimental procedures were approved by The Rockefeller University Animal Care and Use Committee. Male, wild-type, 6- to 7-wk-old C57BL/6 or CD11c*eyfp* transgenic mice (on the C57BL/6 background) were used interchangeably for all experiments. Animals were either bred in The Rockefeller University facilities or purchased from The Jackson Laboratory.

Viral Infection Model. Wild-type VSV, Indiana Serotype (ATCC VR-158) was used in all experiments. Virus purification and the VSV LD_{50} (7,000 pfu) for i.n. administration were determined in 5- to 7-wk-old male mice as described previously (20). For intranasal infection model see *SI Materials and Methods*.

Cytokine Profiling and CORT RIA. VSV-infected animals were killed by rapid decapitation at the indicated time points postinfection. PBS-treated control mice were killed 96 h posttreatment. Cytokines were measured in plasma samples using a BD Cytometric Bead Array Mouse Inflammatory Cytokine Kit (BD Bioscience) according to the manufacturer's protocol and were analyzed immediately on a LSR-II flow cytometer. CORT levels were measured in the plasma of PBS- and VSV-treated animals using the Corticosterone Double Antibody RIA Kit (MP Biomedicals) according to the manufacturer's instructions and were read on a Cobra II Auto-Gamma Counter (Perkin-Elmer).

Quantitative PCR. TaqMan gene-expression assays were used to measure mRNA levels for genes of interest. Eukaryotic 18S rRNA or GAPDH (both from Life Technologies) was used as an internal control. The samples were run on a LightCycler480 real-time PCR thermal cycler (Roche), and the relative ratio of the expression of each gene was calculated using the $2^{-\Delta\Delta Ct}$ method (36). For tissue collection, RNA isolation, and cDNA synthesis, see *SI Materials and Methods*.

Flow Cytometry and FACS. Virally challenged mice were killed 96 hpi by rapid decapitation, and single-cell suspensions were obtained by digestion with collagenase D (Roche), dispase II (Roche), and DNase I (Life Technologies) and repeated trituration using a GentleMACS Dissociator (Miltenyi Biotec). For antibodies and the staining procedure, see *SI Materials and Methods*.

Antagonist Treatment. Mice adjusted to opposite light–dark cycles were treated with the REV-ERBα antagonist SR8278 (Tocris) or vehicle solution in conjunction with VSV. Animal health and survival were monitored daily for 15 d. For gene-expression analysis, mice were killed 12 h after VSV i.n. administration or the last SR8278 treatment. Tissue was extracted and processed for RNA isolation. For detailed treatment procedures and doses used, see *SI Materials and Methods*.

See *SI Materials and Methods* for additional details on the mouse models, antibodies, quantitative PCR (qPCR), immunofluorescence, and the statistics used in this article.

ACKNOWLEDGMENTS. We thank Dr. Paul D'Agostino and Zahrah Masheeb for contributions to the early stages of the study; Dr. Young Cheul Chung and Daniel Cole for technical assistance; and The Rockefeller University's Comparative Bioscience Center, Flow Cytometry Resource Center, and the Bio-Imaging Resource Center for expert technical assistance. This research is supported by a gift from the Peter Deane Trust (to K.B.).

1. Curtis AM, Bellet MM, Sassone-Corsi P, O'Neill LAJ (2014) Circadian clock proteins and immunity. *Immunity* 40(2):178–186.
2. Silver AC, Arjona A, Hughes ME, Nitabach MN, Fikrig E (2012) Circadian expression of clock genes in mouse macrophages, dendritic cells, and B cells. *Brain Behav Immun* 26(3):407–413.
3. Fonken LK, et al. (2015) Microglia inflammatory responses are controlled by an intrinsic circadian clock. *Brain Behav Immun* 45:171–179.
4. Silver AC, Arjona A, Walker WE, Fikrig E (2012) The circadian clock controls toll-like receptor 9-mediated innate and adaptive immunity. *Immunity* 36(2):251–261.
5. Sato S, et al. (2014) A circadian clock gene, Rev-erbα, modulates the inflammatory function of macrophages through the negative regulation of Ccl2 expression. *J Immunol* 192(1):407–417.
6. Sato S, et al. (2014) Direct and indirect suppression of interleukin-6 gene expression in murine macrophages by nuclear orphan receptor REV-ERBα. *ScientificWorldJournal* 2014(5):685854.
7. Gibbs JE, et al. (2012) The nuclear receptor REV-ERBα mediates circadian regulation of innate immunity through selective regulation of inflammatory cytokines. *Proc Natl Acad Sci USA* 109(2):582–587.
8. Hayashi M, Shimba S, Tezuka M (2007) Characterization of the molecular clock in mouse peritoneal macrophages. *Biol Pharm Bull* 30(4):621–626.
9. Yu X, et al. (2013) TH17 cell differentiation is regulated by the circadian clock. *Science* 342(6159):727–730.
10. Arjona A, Boyadjieva N, Sarkar DK (2004) Circadian rhythms of granzyme B, perforin, IFN-gamma, and NK cell cytolytic activity in the spleen: Effects of chronic ethanol. *J Immunol* 172(5):2811–2817.
11. Nguyen KD, et al. (2013) Circadian gene Bmal1 regulates diurnal oscillations of Ly6C(hi) inflammatory monocytes. *Science* 341(6153):1483–1488.
12. Gibbs J, et al. (2014) An epithelial circadian clock controls pulmonary inflammation and glucocorticoid action. *Nat Med* 20(8):919–926.
13. Terry RL, et al. (2012) Inflammatory monocytes and the pathogenesis of viral encephalitis. *J Neuroinflammation* 9(1):270.
14. Shi C, Pamer EG (2011) Monocyte recruitment during infection and inflammation. *Nat Rev Immunol* 11(11):762–774.
15. Geissmann F, et al. (2010) Development of monocytes, macrophages, and dendritic cells. *Science* 327(5966):656–661.
16. Izikson L, Klein RS, Charo IF, Weiner HL, Luster AD (2000) Resistance to experimental autoimmune encephalomyelitis in mice lacking the CC chemokine receptor (CCR)2. *J Exp Med* 192(7):1075–1080.
17. Semple BD, Bye N, Rancan M, Ziebell JM, Morganti-Kossmann MC (2010) Role of CCL2 (MCP-1) in traumatic brain injury (TBI): Evidence from severe TBI patients and CCL2–/– mice. *J Cereb Blood Flow Metab* 30(4):769–782.
18. Hammond MD, et al. (2014) CCR2+ Ly6C(hi) inflammatory monocyte recruitment exacerbates acute disability following intracerebral hemorrhage. *J Neurosci* 34(11):3901–3909.
19. Reiss CS, Plakhov IV, Komatsu T (1998) Viral replication in olfactory receptor neurons and entry into the olfactory bulb and brain. *Ann N Y Acad Sci* 855:751–761.
20. D'Agostino PM, et al. (2012) Viral-induced encephalitis initiates distinct and functional CD103+ CD11b+ brain dendritic cell populations within the olfactory bulb. *Proc Natl Acad Sci USA* 109(16):6175–6180.
21. Trottier MD, Lyles DS, Reiss CS (2007) Peripheral, but not central nervous system, type I interferon expression in mice in response to intranasal vesicular stomatitis virus infection. *J Neurovirol* 13(5):433–445.
22. Cornish TE, Stallknecht DE, Brown CC, Seal BS, Howerth EW (2001) Pathogenesis of experimental vesicular stomatitis virus (New Jersey serotype) infection in the deer mouse (Peromyscus maniculatus). *Vet Pathol* 38(4):396–406.
23. Onishi H, et al. (2002) Rev-erbalpha gene expression in the mouse brain with special emphasis on its circadian profiles in the suprachiasmatic nucleus. *J Neurosci Res* 68(5):551–557.
24. Guilding C, Piggins HD (2007) Challenging the omnipotence of the suprachiasmatic timekeeper: Are circadian oscillators present throughout the mammalian brain? *Eur J Neurosci* 25(11):3195–3216.
25. Kojetin D, Wang Y, Kamenecka TM, Burris TP (2011) Identification of SR8278, a synthetic antagonist of the nuclear heme receptor REV-ERB. *ACS Chem Biol* 6(2):131–134.
26. Chung S, et al. (2014) Impact of circadian nuclear receptor REV-ERBα on midbrain dopamine production and mood regulation. *Cell* 157(4):858–868.
27. Chauhan MB, Chauhan NB (2015) Brain Uptake of Neurotherapeutics after Intranasal versus Intraperitoneal Delivery in Mice. *J Neurol Neurosurg* 2(1):009.
28. Southam DS, Dolovich M, O'Byrne PM, Inman MD (2002) Distribution of intranasal instillations in mice: Effects of volume, time, body position, and anesthesia. *Am J Physiol Lung Cell Mol Physiol* 282(4):L833–L839.
29. Ruzek MC, Miller AH, Opal SM, Pearce BD (1997) Characterization of early cytokine responses and an interleukin (IL)-6–dependent pathway of endogenous glucocorticoid induction during murine cytomegalovirus infection. *J Exp Med* 185(7):1185–1192.
30. Ruzek MC, Pearce BD, Miller AH, Biron CA (1999) Endogenous glucocorticoids protect against cytokine-mediated lethality during viral infection. *J Immunol* 162(6):3527–3533.
31. Rao NAS, et al. (2011) Coactivation of GR and NFKB alters the repertoire of their binding sites and target genes. *Genome Res* 21(9):1404–1416.
32. Dhabhar FS, Malarkey WB, Neri E, McEwen BS (2012) Stress-induced redistribution of immune cells–from barracks to boulevards to battlefields: A tale of three hormones–Curt Richter Award winner. *Psychoneuroendocrinology* 37(9):1345–1368.
33. Dhabhar FS (2014) Effects of stress on immune function: The good, the bad, and the beautiful. *Immunol Res* 58(2-3):193–210.
34. Getts DR, et al. (2008) Ly6c+ "inflammatory monocytes" are microglial precursors recruited in a pathogenic manner in West Nile virus encephalitis. *J Exp Med* 205(10):2319–2337.
35. Tsou C-L, et al. (2007) Critical roles for CCR2 and MCP-3 in monocyte mobilization from bone marrow and recruitment to inflammatory sites. *J Clin Invest* 117(4):902–909.
36. Schmittgen and Livak (2008) Analyzing real-time PCR data by the comperative C_T method. *Nature Protocols* 3(6):1101–1108.